Insect Biochemistry and Molecular Biology 107 (2019) 31–38

Contents lists available at ScienceDirect

Insect Biochemistry and Molecular Biology

journal homepage: www.elsevier.com/locate/ibmb

CRISPR/Cas9-mediated knockout of both the *PxABCC2* and *PxABCC3* genes confers high-level resistance to *Bacillus thuringiensis* Cry1Ac toxin in the diamondback moth, *Plutella xylostella* (L.)

Zhaojiang Guo[1], Dan Sun[1], Shi Kang, Junlei Zhou, Lijun Gong, Jianying Qin, Le Guo, Liuhong Zhu, Yang Bai, Liang Luo, Youjun Zhang*

Department of Plant Protection, Institute of Vegetables and Flowers, Chinese Academy of Agricultural Sciences, Beijing, 100081, China

ARTICLE INFO

Keywords:
Bacillus thuringiensis
Plutella xylostella
CRISPR/Cas9
ABC transporter
Cry1Ac resistance

ABSTRACT

Rapid evolution of resistance by insect pests severely jeopardizes the sustainable utilization of biopesticides and transgenic crops that produce insecticidal crystal proteins derived from the entomopathogenic bacterium *Bacillus thuringiensis* (Bt). Recently, high levels of resistance to Bt Cry1 toxins have been reported to be genetically linked to the mutation or down-regulation of ABC transporter subfamily C genes *ABCC2* and *ABCC3* in seven lepidopteran insects, including *Plutella xylostella* (L.). To further determine the causal relationship between alterations in the *PxABCC2* and *PxABCC3* genes and Cry1Ac resistance in *P. xylostella*, the novel CRISPR/Cas9 genome engineering system was utilized to successfully construct two knockout strains: the ABCC2KO strain is homozygous for a 4-bp deletion in exon 3 of the *PxABCC2* gene, and the ABCC3KO strain is homozygous for a 5-bp deletion in exon 3 of the *PxABCC3* gene, both of which can produce only truncated ABCC proteins. Bioassay results indicated that high levels of resistance to the Cry1Ac protoxin were observed in both the ABCC2KO (724-fold) and ABCC3KO (413-fold) strains compared to the original susceptible DBM1Ac-S strain. Subsequently, dominance degree and genetic complementation tests demonstrated that Cry1Ac resistance in both the knockout strains was incompletely recessive, and Cry1Ac resistance alleles were located in the classic *BtR-1* resistance locus that harbored the *PxABCC2* and *PxABCC3* genes, similar to the near-isogenic resistant NIL-R strain. Moreover, qualitative toxin binding assays revealed that the binding of the Cry1Ac toxin to midgut brush border membrane vesicles (BBMVs) in both knockout strains was dramatically reduced compared to that in the susceptible DBM1Ac-S strain. In summary, our CRISPR/Cas9-mediated genome editing study presents, for the first time, *in vivo* reverse genetics evidence for both the ABCC2 and ABCC3 proteins as midgut functional receptors for Bt Cry1 toxins in insects, which provides new insight into the pivotal roles of both the ABCC2 and ABCC3 proteins in the complex molecular mechanism of insect resistance to Bt Cry1 toxins.

1. Introduction

The pervasive gram-positive soil bacterium *Bacillus thuringiensis* (Bt) is an entomopathogen that generates biodegradable insecticidal toxins (i.e., Cry, Cyt and Vip toxins) during sporulation, which can specifically kill target insect pests but is innocuous to non-target organisms (Schnepf et al., 1998). Therefore, Bt bioinsecticides are considered to be the most successful alternatives to chemical insecticides for controlling insect pests of importance in agriculture, forestry and public health (Bravo et al., 2011). Furthermore, transgenic Bt crops that produce diverse insecticidal toxins have been planted worldwide, and the global cultivation area reached more than 100 million hectares in 2017, which is of great significance for pest suppression and insecticide reduction in fields (ISAAA, 2017). Nonetheless, the widespread adoption of Bt sprays and Bt crops inevitably imposes intense selective pressure for insect pests to develop field-evolved Bt resistance, thereby diminishing the benefits provided by Bt biotechnology. Currently, field-evolved Bt resistance has been documented in at least eight lepidopteran and one

* Corresponding author. Department of Plant Protection, Institute of Vegetables and Flowers, Chinese Academy of Agricultural Sciences, No.12, Zhongguancun South Street, Haidian District, Beijing, 100081, China.

E-mail addresses: guozhaojiang@caas.cn (Z. Guo), sun13804560684@163.com (D. Sun), kangshi0718@163.com (S. Kang), zhoujunlei2006@126.com (J. Zhou), gonglijun025@163.com (L. Gong), qinjianying0203@163.com (J. Qin), guole930323@163.com (L. Guo), liuhongzhu1992@126.com (L. Zhu), baiyang15765533722@163.com (Y. Bai), luoliang10090419@163.com (L. Luo), zhangyoujun@caas.cn (Y. Zhang).

[1] Both authors contributed equally to this work.

https://doi.org/10.1016/j.ibmb.2019.01.009
Received 23 November 2018; Received in revised form 18 December 2018; Accepted 29 January 2019
Available online 30 January 2019

coleopteran insect (Bravo et al., 2011; Tabashnik and Carrière, 2017). In this regard, a comprehensive understanding of the molecular mechanisms underlying Bt resistance in different insects is required for sustainable utilization of Bt products.

Extensive studies have established the current mode of action of three-domain Bt Cry toxins in the insect midgut epithelium: after ingestion by susceptible insects, Bt Cry protoxins are solubilized in the midgut fluids and are digested by midgut proteases to yield activated Cry toxins. The activated Cry toxins then traverse the peritrophic matrix and reach the brush border membrane of the midgut epithelium. The Cry toxins undergo further proteolysis to form prepore oligomers and sequentially bind to multiple midgut membrane receptors, resulting in pore formation in the membrane and insect death (Pardo-López et al., 2013). In this sequential binding model, specific toxin-receptor interaction is pivotal for toxicity, and alteration of these midgut receptors confers high levels of Bt resistance in insects (Adang et al., 2014; Peterson et al., 2017). To date, myriad midgut membrane receptors of Bt Cry toxins have been identified, such as classical cadherin, alkaline phosphatase (ALP), and aminopeptidase (APN) (Pigott and Ellar, 2007). Recently, versatile ABC transporters have received much attention from insect toxicologists due to the involvement of these proteins in Bt resistance in various insects because these proteins can also act as functional midgut membrane receptors for Cry toxins (Heckel, 2012; Tanaka et al., 2013).

The diamondback moth, *Plutella xylostella* (L.), is a notorious global pest that infests *Brassica* vegetables and oilseed crops, and the damage caused by this insect is now estimated to cost the world economy US$4-5 billion annually (Furlong et al., 2013). Notably, this insect was the first and only pest that developed resistance to Bt sprays in open fields (Tabashnik et al., 1990), rendering it a model insect for investigation of the molecular basis of insect resistance to Bt Cry toxins. Previously, Bt Cry1Ac resistance in *P. xylostella* has been confirmed to be genetically linked to *cis*-mutation of the *PxABCC2* gene (Baxter et al., 2011). Nevertheless, despite the parallel evolution (Baxter et al., 2011), many pathways have led to successfully adaption by *P. xylostella*, and resistance to the Cry1Ac toxin can be a feasible direction for adaptive evolution in fields. For instance, our recent molecular and genetic studies have shown that down-regulation of the *PxmALP*, *PxABCC2*, *PxABCC3* and *PxABCG1* genes is also closely associated with Cry1Ac resistance in *P. xylostella* (Guo et al., 2015a, 2015c), and the emerging omics-based approaches have identified many other potential differentially expressed genes or Cry1Ac-binding proteins that might be correlated with Cry1Ac resistance in *P. xylostella* (Xie et al., 2012; Lei et al., 2014; Ayra-Pardo et al., 2015; Xia et al., 2016; Zhu et al., 2016a). Apparently, the molecular mechanisms underlying the resistance *P. xylostella* to Bt Cry1Ac toxin are complex and multifaceted, and numerous midgut genes are possibly associated with Cry1Ac resistance in *P. xylostella*, while the precise roles of these genes in Cry1Ac resistance remain to be further unraveled (Crickmore, 2016). Hence, direct *in vivo* functional evidence is urgently needed to definitively identify the causal link between alterations in these candidate functional genes and Cry1Ac resistance in *P. xylostella*.

The novel clustered regularly interspaced short palindromic repeats (CRISPR)/CRISPR-associated protein 9 (Cas9) technology that originated from the adaptive defense systems of bacteria and archaea has been developed as a powerful genetic manipulation tool (Jinek et al., 2012; Hsu et al., 2014). This system relies mainly on a single guide RNA (sgRNA) chimera of mature CRISPR RNA (crRNA) and *trans*-activating crRNA (tracrRNA), which is combined with Cas9 to cleave complementary target DNA sequences adjacent to a protospacer adjacent motif (PAM), thereby creating a double-strand break (DSB), and targeted genome modifications are obtained via non-homologous end-joining (NHEJ) or homology-directed repair (HDR) of the regions flanking the cleavage site (Knott and Doudna, 2018). To date, the CRISPR/Cas9 genome editing system has been used for precise genome editing to study gene functions in many insects and other arthropods (Sun et al., 2017). Although alterations in the *ABCC2* and *ABCC3* genes have been documented to be associated with Bt resistance in seven lepidopteran insects including *P. xylostella* (Gahan et al., 2010; Baxter et al., 2011; Atsumi et al., 2012; Park et al., 2014; Xiao et al., 2014; Guo et al., 2015a; Banerjee et al., 2017; Flagel et al., 2018), functional validation of both ABC transporter genes in Bt resistance by the CRISPR/Cas9 system has not yet been reported. In particular, the PxABCC2 protein has been recently verified *in vitro* to be involved in Cry1Ac toxin oligomerization and membrane insertion in *P. xylostella* (Ocelotl et al., 2017). Accordingly, it is plausible to conclude that PxABCC2 and even its paralog PxABCC3 are crucial midgut receptors for Cry1Ac toxin to mediate toxicity in *P. xylostella*. However, further *in vivo* functional studies by utilizing the novel CRISPR/Cas9 technique are still required to provide definitive evidence of the important role of the *PxABCC2* and *PxABCC3* genes in the Cry1Ac resistance of *P. xylostella*.

In this study, CRISPR/Cas9-mediated knockout of both the *PxABCC2* and *PxABCC3* genes was conducted from the Cry1Ac-susceptible DBM1Ac-S strain of *P. xylostella*, and two knockout strains exhibited high levels of resistance to the Cry1Ac protoxin. Our results provide conclusive *in vivo* functional evidence that both the PxABCC2 and PxABCC3 proteins can serve as midgut functional receptors of Cry1Ac toxin, and disruption of both ABC transporter genes can confer high-level Cry1Ac resistance to *P. xylostella*.

2. Materials and methods

2.1. Insect strains

The Bt Cry1Ac-susceptible *P. xylostella* strain DBM1Ac-S and its near-isogenic field-evolved Cry1Ac-resistant *P. xylostella* strain NIL-R used in this study have been described in detail previously (Guo et al., 2015b; Zhu et al., 2015, 2016b). Additionally, via CRISPR/Cas9-mediated knockout of both the *PxABCC2* and *PxABCC3* genes (GenBank accession nos. KM245561 and KM245562) in DBM1Ac-S, we established two new strains that were designated ABCC2KO and ABCC3KO, which are homozygous for 4-bp and 5-bp deletions in exon 3 of the *PxABCC2* and *PxABCC3* genes, respectively. All four *P. xylostella* strains were reared *en masse* on Jing Feng No. 1 cabbage (*Brassica oleracea* var. *capitata*) at 25 °C with 65% relative humidity (RH) and a 16:8 (light:-dark) photoperiod, and adults were supplied with a 10% honey/water solution.

2.2. Cry1Ac toxin preparation

Both Cry1Ac protoxin and trypsin-activated Cry1Ac toxin were prepared as mentioned previously (Guo et al., 2015c, d). The Cry1Ac toxin preparations were dissolved in 50 mM Na_2CO_3 (pH 9.6) and stored at −20 °C until needed.

2.3. sgRNA design and synthesis

The optimized sgRNA target sequences were both designed in exon 3 of the *PxABCC2* and *PxABCC3* genes (Fig. 2A and E) via the CRISPR RGEN tool Cas-Designer (http://www.rgenome.net/cas-designer/); these regions are gene-specific transmembrane domains (TM2 domains), avoiding posttranscriptional alternative splicing as previously reported (Guo et al., 2015a). The potential off-target effects of both the selected sgRNA target sequences were eliminated by searching the *P. xylostella* genome database (DBM-DB, http://59.79.254.1/DBM/index.php) and GenBank database (https://www.ncbi.nlm.nih.gov/) combined with the CRISPR RGEN tool Cas-OFFinder (http://www.rgenome.net/cas-offinder/). To prepare the template DNA for *in vitro* sgRNA synthesis, fusion PCR was then performed with two oligonucleotides using the high-fidelity PrimeSTAR Max DNA polymerase (TaKaRa, Dalian, China); one specific oligonucleotide was regarded as the forward primer and encoded the T7 polymerase binding site (italicized)

and the sgRNA target sequence (GN_{19}, underlined) of each gene (CRISPR-C2-F: 5′-*GAAATTAATACGACTCACTATAGG*GCTGTGCAACTTCCTGGCCAGTTTTAGAGCTAGAAATAGC-3′, CRISPR-C3-F: 5′-*GAAATTAATACGACTCACTATAGG*GTACTACACGGTGGGCATGGGTTTTAGAGCTAGAAATAGC-3′), and the other common oligonucleotide served as the reverse primer and encoded the remaining sgRNA sequences (CRISPR-R: 5′-AAAAGCACCGACTCGGTGCCACTTTTTCAAGTTGATAACGGACTAGCCTTATTTTAACTTGCTATTTCTAGCTCTAAAAC-3′). The hybridization PCR (in a total volume of 50 μl) contained 25 μl of PrimeSTAR Max Premix (2×), 2 μl of CRISPR-C2/C3-F (10 μM), 2 μl of CRISPR-R (10 μM) and 21 μl of ddH_2O. The PCR program was conducted with the following parameters: one cycle of 98 °C for 2 min; 38 cycles of 98 °C for 10 s, 70 °C for 5 s and 72 °C for 30 s; and a final cycle of 72 °C for 10 min. The PCR products were purified with the DNA Clean-up Kit (CWBIO, Beijing, China). The purity and concentration of the generated DNA templates were detected with a NanoDrop 2000c spectrophotometer (Thermo Fisher Scientific, Waltham, MA, USA). Whereafter, *in vitro* transcription was performed to produce the sgRNAs with the MEGAscript Transcription Kit (Ambion, Foster City, CA, USA) following the manufacturer's protocol, and the generated sgRNAs were further purified by the MEGAclear Kit (Ambion, Foster City, CA, USA). The synthesized sgRNA samples were used immediately or stored in aliquots at −80 °C until use.

2.4. Cas9 protein

The recombinant Cas9 protein from *Streptococcus pyogenes* used in this study was obtained commercially (Thermo Fisher Scientific, Waltham, MA, USA).

2.5. Embryo collection and microinjection

Fresh preblastoderm-stage eggs were collected on dry microscope slides (24 × 50 mm), which were precoated with fresh cabbage leaf juice to induce the oviposition behavior of female adults. Mixtures of Cas9 (300 ng/μl) and sgRNA (150 ng/μl) were injected into the germ cells located at the posterior pole of each egg within 2 h after oviposition using a FemtoJet 4i and an InjectMan 4 microinjection system (Eppendorf, Hamburg, Germany) attached to glass needles (Sutter Instrument, Novato, CA, USA) pulled by a P-97 micropipette puller (Sutter Instrument, Novato, CA, USA) and polished by an EG-401 microgrinder (Narishige, Tokyo, Japan). The injected eggs were immediately returned to normal rearing conditions for hatching.

2.6. gDNA isolation and mutagenesis detection

To genotype the indel (insertion or deletion) mutations of both the *PxABCC2* and *PxABCC3* genes induced by the CRISPR/Cas9 genome editing system (Fig. 1A), genomic DNA (gDNA) samples were extracted from tiny exuviates of the final fourth-instar *P. xylostella* larvae (Fig. 1B), which is an effective and nondestructive method that is used to avoid damaging the pupae, as reported elsewhere (Wang et al., 2016). Trace amounts of gDNA were isolated individually using the KAPA Express Extract DNA Extraction Kit (KAPA Biosystems, Boston, MA, USA) according to the manufacturer's recommendations. Then, the gDNA fragments of both *PxABCC2* (305 bp) and *PxABCC3* (298 bp) (Fig. 1C) were amplified by PCR using the corresponding gene-specific primer pairs flanking the sgRNA target sites (ABCC2-F: 5′-TTGTTGATCAAACTTGCCCTAC-3′, ABCC2-R: 5′-CTTCCGATACACATACCTTA-3′; ABCC3-F: 5′-CACGGAATCATCTTACGGTT-3′, ABCC3-R: 5′-GTAAGTACCAGATTTGCTAA-3′). The PCRs (in a total volume of 25 μl) contained 12.5 μl of PrimeSTAR Max premix (2×), 0.5 μl of ABCC2/C3-F (10 μM), 0.5 μl of ABCC2/C3-R (10 μM), 150 ng of gDNA template and 10.5 μl of ddH_2O. The PCR program was as follows: one cycle of 98 °C for 2 min; 35 cycles of 98 °C for 10 s, 55 °C for 15 s and 72 °C for 30 s; and a final cycle of 72 °C for 10 min. The final PCR products were directly sequenced using the forward primer of each gene as the sequencing primer. The sequencing chromatograms displaying double peaks flanking the Cas9 cutting site of each gene demonstrated heterozygotes harboring monoallelic or biallelic mutation, and these PCR products were further ligated into the *pEASY*-T1 cloning vector and sequenced for exact indel mutation type detection.

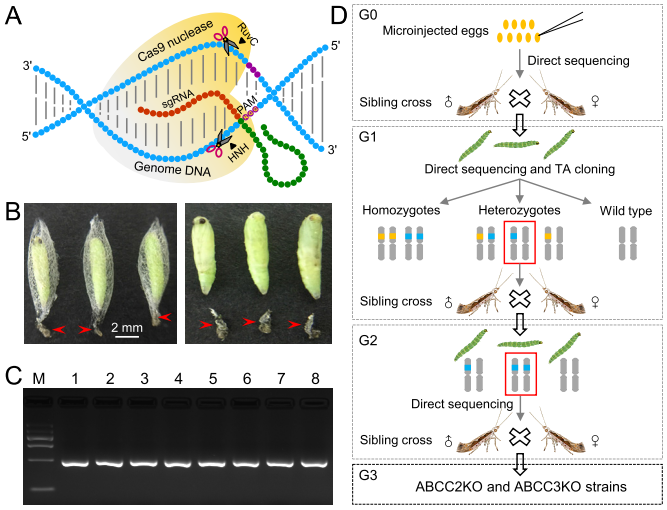

Fig. 1. The strategy for genome engineering using the CRISPR/Cas9 system for gene knockout in *P. xylostella*. (A) The architecture of the CRISPR/Cas9 genome editing system. The sgRNA could interact with Cas9 nuclease to recognize the PAM site (NGG) in the target DNA strand and direct Cas9 to cleave dsDNA via the HNH and RuvC nuclease domains. (B) The tiny exuviates of the final fourth-instar *P. xylostella* larvae in each generation (red arrows) used for individual gDNA extraction and subsequent gene mutation detection. (C) The gDNA fragments of *PxABCC2* (305 bp, lanes 1-4) and *PxABCC3* (298 bp, lanes 5-8) were successfully cloned using the gDNA sample extracted from a single exuviate of fourth-instar larvae and resolved on 2% agarose gels. Lane M: DNA marker. (D) A flow diagram of the detailed crossing scheme used in this study to obtain the homozygous *PxABCC2* and *PxABCC3* knockout strains. CRISPR/Cas9-induced gene mutations were identified by direct sequencing, and different mutant genotypes were further detected by TA cloning and sequencing in G1 individuals. For these genotypes, gray columns represent autosomes, and the boxes with different colors denote the autosomal regions with a disrupted *PxABCC2* or *PxABCC3* gene. (For interpretation of the references to color in this figure legend, the reader is referred to the Web version of this article.)

2.7. Homozygous mutant strain construction

To construct stable homozygous mutant strains of both the *PxABCC2* and *PxABCC3* genes, a germline transformation and mutation screening strategy was developed and optimized (Fig. 1D). G0 generation larvae were obtained by microinjecting a mixture of Cas9 protein and sgRNA targeting the *PxABCC2* or *PxABCC3* genes into preblastoderm eggs. The mutant moths verified by direct sequencing were in-crossed to obtain G1 offspring, and the specific indel mutated alleles were identified based on positive direct sequencing results and subsequent TA cloning and sequencing results in G1. Sufficient heterozygous individuals with the same allelic mutation of each gene were selected, and the moths from each group were sibling crossed to obtain G2 progeny. The G2 individuals containing homozygous mutant alleles were screened again by direct sequencing, and the mutant homozygotes were mass crossed to establish the stable homozygous mutant ABCC2KO and ABCC3KO strains in G3.

2.8. Insect bioassays

Leaf-dip bioassays were performed to determine the toxicity of the DBM1Ac-S, NIL-R, ABCC2KO and ABCC3KO strains to Bt Cry1Ac

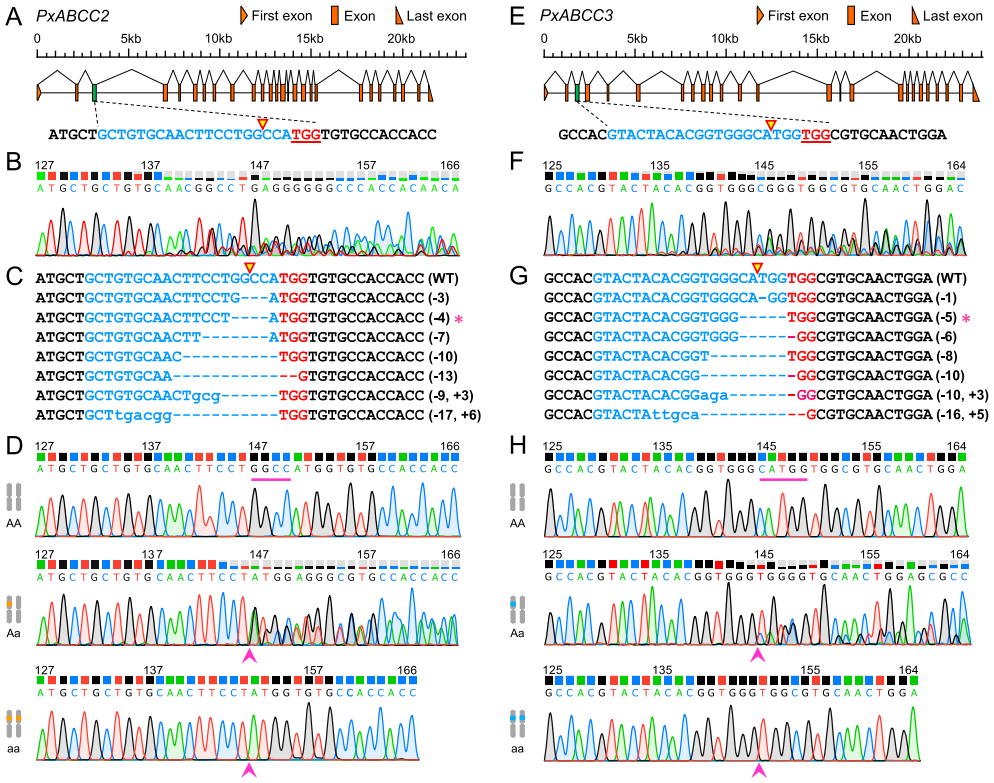

Fig. 2. CRISPR/Cas9-mediated sequence-specific mutation types of *PxABCC2* and *PxABCC3* in *P. xylostella*. (A) and (E) The designed sgRNA-targeted sites and sequences in exon 3 (green boxes) of both *PxABCC2* (A) and *PxABCC3* (E). The genomic structures of both genes are drawn to scale. Exons are shown as boxes and triangles, and the spaces between two exons indicate the introns. The sgRNA target sequences of both genes are highlighted in blue; the PAM sequences are marked in red and underlined; and the cleavage site is indicated with a red-edged yellow inverted triangle. (B) and (F) Representative direct sequencing chromatograms of the pooled PCR products from mutated G0 individuals of both *PxABCC2* (B) and *PxABCC3* (F) with a stretch of typical multiple peaks. (C) and (G) Various types of indel mutations flanking the CRISPR target sites of *PxABCC2* (C) and *PxABCC3* (G) exhibited by G1 larvae, as identified by TA cloning and sequencing of the individual PCR products. Among these different mutant genotypes, the deleted bases are shown as dashes, and the inserted bases are indicated with lowercase letters. The numbers of inserted or deleted bases are displayed at the right of each allele (+, insertion; –, deletion). Asterisks denote the selected monoallelic mutants with enough individuals used for further sib-crossing to generate G2 strains. (D) and (H) Representative chromatograms of direct sequencing of the PCR products derived from wild types (upper graph), mutant heterozygotes (middle graph) and mutant homozygotes (lower graph) of both *PxABCC2* (D) and *PxABCC3* (H) in G2 individuals. The locations of CRISPR/Cas9-induced 4-bp deletion (GGCC) within exon 3 of *PxABCC2* and 5-bp deletion (CATGG) within exon 3 of *PxABCC3* are marked by pink lines and arrows. (For interpretation of the references to color in this figure legend, the reader is referred to the Web version of this article.)

protoxin as described previously (Guo et al., 2015c). Briefly, ten early third-instar larvae were tested for each of the seven gradient dilutions of toxin concentrations, and the bioassays were repeated in quadruplicate. Larval mortality was recorded after 72 h before pupation, and the control mortality did not exceed 5%. Larvae were considered as dead if they died or displayed severe growth retardation at the end of the bioassays. After toxicity bioassays, the LC_{50} (median lethal concentration that killed 50% of the tested larvae) and 95% CL (95% confidence limits of the LC_{50}) values were both calculated by probit analysis using POLO Plus 2.0 software (LeOra Software, Berkeley, CA, USA). Two compared LC_{50} values with nonoverlapping 95% CL values were considered to be significantly different, and the resistance ratios were calculated by dividing the LC_{50} value for each strain by the LC_{50} value for the susceptible DBM1Ac-S strain.

2.9. Dominance degree and genetic complementation tests

To determine the dominance degree and allelism of the Cry1Ac resistance phenotype in both knockout strains, virgin males and females of the DBM1Ac-S, ABCC2KO, ABCC3KO and NIL-R strains were visually separated upon emergence, and mass interstrain crossing (50 pairs) was performed between two out of these four strains. The toxicity responses of these four strains and their F1 progeny were tested at a discriminating concentration (10 mg/L) of Cry1Ac protoxin, killing 100% of the completely recessive heterozygous F1 larvae, and the sample sizes to obtain the survival or mortality rates were 50 larvae for each strain and 100 larvae for each F1 offspring. Based on the single-concentration method described elsewhere (Liu and Tabashnik, 1997), the dominance (*h*) of Cry1Ac resistance was calculated as (the survival rate of F1 hybrid progeny – the survival rate of DBM1Ac-S) divided by (the survival rate of resistant strain – the survival rate of DBM1Ac-S), with values ranging from 0 (complete recessivity) to 1 (complete dominance). For the interstrain allelic complementation test, if the recessive resistance alleles were located at the same locus in two parent strains, the F1 progeny of these strains was resistant to Cry1Ac toxin. If the recessive resistance alleles occurred at different loci in these two crossed strains, the F1 progeny of these strains exhibited allelic complementation, thereby restoring the susceptibility to the Cry1Ac toxin.

2.10. BBMV preparation and Cry1Ac binding assays

To further test the influence of both the *PxABCC2* and *PxABCC3* gene knockouts on the binding of the Cry1Ac toxin to larval midgut epithelial cells, midgut brush border membrane vesicles (BBMV) were prepared, and Cry1Ac binding assays were conducted as described previously (Guo et al., 2015a), with slight modifications. First, midgut tissues of fourth-instar *P. xylostella* larvae were dissected, and BBMV samples were isolated in ice-cold MET buffer [17 mM Tris–HCl (pH 7.5), 5 mM EGTA, 300 mM mannitol] plus protease inhibitors (1 mM PMSF) using the differential magnesium precipitation method. Then, the purified BBMV proteins were quantified using the Bradford method with bovine serum albumin (BSA) as a standard, and the proteins were used immediately or kept in aliquots at −80 °C until use. A between 5 and 8-fold increase in specific APN activity using L-leucine-*p*-nitroanilide (Sigma, St. Louis, MO, USA) as a substrate was observed in the final BBMV samples compared to the initial midgut homogenates. Subsequently, qualitative binding of trypsin-activated Cry1Ac toxin to BBMV samples was monitored by Western blotting. BBMV samples (10 μg) were incubated with Cry1Ac toxin (10 nM) in 100 μl of PBS binding buffer [1 × PBS (137 mM NaCl, 2.7 mM KCl, 10 mM Na_2HPO_4, 2.0 mM KH_2PO_4), 0.1% BSA and 0.1% Tween-20, pH 7.6] at room temperature for 1 h. After incubation, the binding reaction was terminated by centrifugation at 20000 × *g* for 10 min at 4 °C, and the resulting pellets were washed and centrifuged three times with 0.5 ml of ice-cold

PBS binding buffer to remove unbound Cry1Ac toxin. The final collected BBMV pellets were resuspended in SDS-PAGE loading buffer and boiled for 5 min. Then, the BBMV samples were separated by 10% SDS-PAGE and electroblotted onto Immobilon-P polyvinylidene difluoride (PVDF) membranes (Merck Millipore, Bedford, MA, USA) in Towbins's transfer buffer (25 mM Tris, 192 mM glycine, 0.1% SDS, 20% methanol, pH 8.3) with a constant current of 300 mA at 4 °C for 1 h. The PVDF filters were then incubated with BSA blocking buffer (1 × PBS, 0.1% Tween-20, 3% BSA) for 1 h with constant shaking. Cry1Ac toxin binding was detected by incubation with our previously produced rabbit anti-Cry1Ac polyclonal antiserum (1:100000) followed by a horseradish peroxidase (HRP)-conjugated goat anti-rabbit secondary antibody (1:5000) (CWBIO, Beijing, China) at room temperature for 1 h. The bound Cry1Ac toxin was visualized using the SuperSignal West Pico chemiluminescent substrate (Thermo Fisher Scientific, Waltham, MA, USA) and photographed with the Tanon-5200 chemiluminescence imaging system (Tanon, Shanghai, China). Relative binding of Cry1Ac toxin was quantified by densitometry using ImageJ v.1.51 software (http://rsbweb.nih.gov/ij/) with the intensity of the DBM1Ac-S BBMV sample assigned an arbitrary value of 100%. The data presented are the means and the corresponding standard errors from three biological replicates.

3. Results

3.1. Establishment of homozygous PxABCC2 and PxABCC3 knockout strains

A total of 215 and 200 fresh preblastoderm eggs from the *P. xylostella* strain DBM1Ac-S were successively microinjected with a mixture of Cas9 proteins and the sgRNAs targeting exon 3 of *PxABCC2* (Fig. 2A) and *PxABCC3* (Fig. 2E), respectively. For the *PxABCC2* group (group 1), approximately 65% (140/215) of the injected eggs hatched to larvae, and 57% (80/140) of the larvae successfully developed to adults (G0). In the *PxABCC3* group (group 2), approximately 60% (120/200) of the injected eggs hatched to larvae, and 57% (68/120) of the larvae successfully developed to adults (G0). Meanwhile, nondestructive genotyping of indel mutations around the sgRNA target site was conducted using PCR with gDNA samples prepared from exuviates of individual fourth-instar G0 larvae of each group as templates. Direct sequencing of individual PCR products showed that high site-specific mutagenic efficiency of 65% (52/80) and 59% (40/68) was induced in groups 1 and 2 by the CRISPR/Cas9 system, which was also confirmed by the direct sequencing chromatogram of the pooled PCR products with a cluster of multi-peaks at each CRISPR target site (Fig. 2B and F). Subsequently, the screened G0 male and female moths with mutant alleles were mass crossed to produce the next generation (G1) in each group.

The G1 larvae were reared to pupae, and approximately 111 fourth-instar larvae from group 1 and 96 fourth-instar larvae from group 2 were randomly selected (sex ratio = 1:1) for mutation scanning. Direct sequencing and further TA cloning and sequencing of G1 individual exuviates revealed seven different types of indel mutations in each group (Fig. 2C and G), suggesting that the genome-edited gene alleles in both groups could be transmitted to the next generation. In group 1, the 111 genotyped G1 individuals included 61 wild-type homozygotes, 11 biallelic heterozygous mutants and 39 monoallelic mutants. Among these individuals, the 39 monoallelic mutants included 7 different mutation types, including type A (n = 11, with a 3-bp deletion), type B (n = 16, with a 4-bp deletion), type C (n = 3, with a 7-bp deletion), type D (n = 3, with a 10-bp deletion), type E (n = 2, with a 13-bp deletion), type F (n = 3, with a 9-bp deletion and 3-bp insertion), type G (n = 1, with a 17-bp deletion and 6-bp insertion) (Fig. 2C). In group 2, the 96 genotyped G1 individuals included 53 wild-type homozygotes, 8 biallelic heterozygous mutants and 35 monoallelic mutants. Among these individuals, the 35 monoallelic mutants also included 7 different mutation types, including type A (n = 9, with a 1-bp deletion), type B (n = 17, with a 5-bp deletion), type C (n = 3, with a 6-bp deletion), type D (n = 2, with an 8-bp deletion), type E (n = 1, with a 10-bp deletion), type F (n = 1, with a 10-bp deletion and 3-bp insertion), type G (n = 2, with a 16-bp deletion and 5-bp insertion) (Fig. 2G). In both G1 groups, type B contained the largest number of individuals with a nearly 1:1 sex ratio, so we mass crossed the male and female moths from type B in each group to further generate enough G2 progeny and transmit the mutant allele to G2.

More than 100 G2 individuals in each group were genotyped by direct sequencing using the gDNA samples from randomly selected exuviates of the final fourth-instar larvae (Fig. 2D and H). The sequencing results showed that approximately 16% (19/119) were homozygous for the 4-bp deletion at exon 3 of *PxABCC2* and that approximately 18% (23/127) were homozygous for the 5-bp deletion at exon 3 of *PxABCC3* (Fig. 2D and H). The 19 homozygous mutants (9 males and 10 females) from group 1 were sib-crossed to create the stable homozygous mutant strain ABCC2KO in G3, and the 23 homozygous mutants (10 males and 13 females) from group 2 were also sib-crossed to create another stable homozygous mutant strain ABCC3KO in G3.

3.2. Resistance to Cry1Ac protoxin caused by PxABCC2 and PxABCC3 knockouts

Previous studies have demonstrated that deletion mutation of *PxABCC2* or reduced expression of *PxABCC2* and *PxABCC3* is genetically linked to high-level Cry1Ac resistance in *P. xylostella* (Baxter et al., 2011; Guo et al., 2015a). For further *in vivo* determination of whether both *PxABCC2* and *PxABCC3* are involved in Cry1Ac resistance in *P. xylostella*, two stable knockout strains of *PxABCC2* and *PxABCC3* were established using the novel powerful CRISPR/Cas9 genome editing system as described above, wherein the deletion mutations were predicted to truncate the PxABCC2 or PxABCC3 proteins.

Susceptibility to the Cry1Ac protoxin was tested in the two knockout strains with the original susceptible strain DBM1Ac-S as a negative control and its near-isogenic resistant strain NIL-R as a positive control. As expected, the bioassay results indicated that the LC_{50} values of the ABCC2KO strain [535.49 (409.59–749.18) mg/L], ABCC2KO strain [305.75 (240.12–397.79) mg/L] and NIL-R strain [3778.64 (2710.88–5602.84) mg/L] to the Cry1Ac protoxin were approximately 724-, 413- and 5106-fold higher, respectively, than that of the near-isogenic susceptible DBM1Ac-S strain [0.74 (0.58–0.95) mg/L] (Fig. 3A). Intriguingly, both knockout strains exhibited high levels of resistance to the Cry1Ac protoxin, but the resistance level in ABCC2KO was significantly higher than that in ABCC3KO, albeit not as high as the extremely high resistance of the NIL-R strain to the Cry1Ac protoxin (Fig. 3A). Our bioassay results presented strong *in vivo* functional evidence that both the PxABCC2 and PxABCC3 proteins can function as midgut functional receptors of Cry1Ac toxin in *P. xylostella*, but compared to PxABCC2, PxABCC3 is a relatively low-functioning Cry1Ac receptor that mediates toxicity.

3.3. Genetic analysis of Cry1Ac resistance phenotypes in both knockout strains

To determine the mode of inheritance of Cry1Ac resistance in both knockout strains, interstrain crossing was performed between pairs of strains from DBM1Ac-S, ABCC2KO, ABCC3KO and NIL-R, and the responses of these four strains and their F1 progeny were examined with a diagnostic dose (10 mg/L) of the Cry1Ac protoxin. The diagnostic dose of the Cry1Ac protoxin (10 mg/L) could kill all the susceptible DBM1Ac-S larvae and nearly all the incompletely recessive heterozygous F1 hybrids (86%), whereas this dose could not kill the resistant NIL-R larvae (Fig. 3B). Similar to the dominance degree (h = 0.14) for the NIL-R strain, the dominance parameters (h) for the two resistant knockout strains were 0.16 and 0.15, indicating that the Cry1Ac

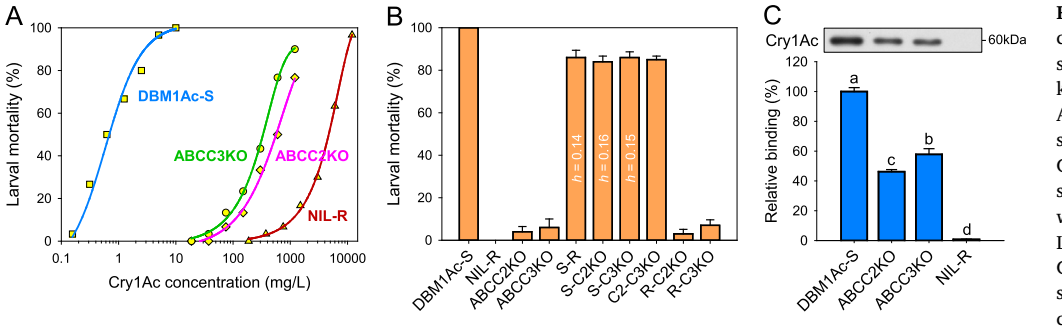

Fig. 3. (A) Nonlinear log dose-response curves for *P. xylostella* larvae from the susceptible strain DBM1Ac-S, two knockout strains ABCC2KO and ABCC3KO, and the near-isogenic resistant strain NIL-R exposed to the Cry1Ac protoxin. Two nonlinear dosage-mortality regression curves without intersections represent two LC_{50} values with nonoverlapping 95% CL values, which can be considered significantly different. (B) Interstrain complementation tests for allelism with diagnostic doses of Cry1Ac protoxin. F_1 progeny are produced by crossing one susceptible and three resistant strains in all pairwise combinations, and the dominance parameter *h* of each crossed group is shown on the column. (C) Decreased Cry1Ac binding in resistant BBMVs compared to their susceptible counterpart. Both bound toxin detection by Western blotting (upper row) and binding quantification by densitometry (lower graph) are shown. The percentage of binding is relative to data calculated from three independent DBM1Ac-S BBMV samples. Error bars in each column indicate standard errors of the mean (SEMs) from three biological repeats, and different letters on the bars denote dramatic differences in Cry1Ac binding among strains ($P < 0.05$; Duncan's test; $n = 3$).

resistance traits were also incompletely recessive for both resistant knockout strains (Fig. 3B). As expected, the F1 progeny from the mass cross between ABCC2KO and ABCC3KO resistant strains had a high mortality rate (85%) at 10 mg/L Cry1Ac protoxin, while the F1 progeny from the mass cross between ABCC2KO or ABCC3KO and NIL-R resistant strains had low mortality rates (3% and 7%) at this diagnostic concentration of Cry1Ac protoxin (Fig. 3B). The interstrain allelic complementation test confirmed that Cry1Ac resistance is conferred by the *BtR-1* resistance locus that harbors the *PxABCC2* and *PxABCC3* genes in both resistant knockout strains, similar to the NIL-R strain.

3.4. Reduced Cry1Ac toxin binding to midgut BBMVs in both knockout strains

Qualitative binding of the Cry1Ac toxin to the midgut BBMV samples was detected *in vitro* by Western blotting for the DBM1Ac-S, ABCC2KO, ABCC3KO and NIL-R strains. Consistent with our previous observation (Guo et al., 2015a), the Cry1Ac toxin could bind to the midgut BBMV proteins in the susceptible DBM1Ac-S strain, while nearly complete loss of binding of the toxin to the midgut BBMV proteins was observed in the high-level resistant NIL-R strain (Fig. 3C). In contrast, significantly reduced binding of the Cry1Ac toxin to midgut BBMV proteins was detected in both resistant knockout strains, with a relatively higher degree of reduction observed in ABCC2KO than in ABCC3KO ($P < 0.05$; Duncan's tests; $n = 3$) (Fig. 3C). The Cry1Ac toxin binding assays demonstrated that disruption of both the *PxABCC2* and *PxABCC3* genes resulted in decreased Cry1Ac binding, thereby conferring high levels of Cry1Ac toxin resistance to *P. xylostella*, and the increased loss of Cry1Ac binding correlated well with the increased resistance ratio of the ABCC2KO strain compared to the ABCC3KO strain.

4. Discussion

The currently available powerful CRISPR/Cas9 system enables us to validate gene functions with high efficiency and accuracy in different insects, especially in non-model agricultural pests (Sun et al., 2017). Based on the indel mutations of target genes that were directly introgressed into a controlled genetic background, we can obtain an accurate *in vivo* estimation of gene functions associated with certain phenotypes in insects. To utilize this novel technology in the study of Bt resistance in *P. xylostella*, we overcame the challenge posed by invisible loss-of-function mutation phenotypes by developing a practical and nondestructive method to effectively discriminate among the genotypes, which necessitated isolation of individual gDNA samples from tiny exuviates of the final fourth-instar *P. xylostella* larvae as previously reported in *Helicoverpa armigera* (Wang et al., 2016). Ultimately, both the *PxABCC2* and *PxABCC3* genes were successfully knocked out by the CRISPR/Cas9 system in the Cry1Ac-susceptible DBM1Ac-S strain of *P. xylostella*.

As expected, both the knockout strains ABCC2KO and ABCC3KO exhibited high-level resistance to Cry1Ac protoxin, suggesting that both the PxABCC2 and PxABCC3 proteins can act as functional midgut receptors for Cry1Ac toxin in *P. xylostella*. However, the resistance level of ABCC2KO (724-fold) was strikingly higher than that of ABCC3KO (413-fold), demonstrating that the contribution of PxABCC2 disruption to Cry1Ac resistance was much higher than that of PxABCC3. Indeed, our previous study also found that reduced expression of the *PxABCC2* gene was markedly higher than that of the *PxABCC3* gene in the resistant NIL-R strain, and silencing of the *PxABCC2* gene in the susceptible DBM1Ac-S strain can result in a greater decrease in larval susceptibility to Cry1Ac protoxin than silencing of the *PxABCC3* gene (Guo et al., 2015a). Moreover, the results here are consistent with a recent study on the *SeABCC2* and *SeABCC3* genes of *Spodoptera exigua*, which indicated that ectopic expression of the *SeABCC2* gene conferred relatively lower Cry1Aa susceptibility to HEK293T cells than ectopic expression of the *SeABCC3* gene (Endo et al., 2017). Recently, the same research group revealed that the recombinant *Bombyx mori* ABCC3 (BmABCC3) protein exhibited distinctly lower binding affinities to both the Cry1Aa and Cry1Ab toxins than BmABCC2 in HEK293T cells (Endo et al., 2018). As a corollary, the Cry1Ac binding affinity of PxABCC3 could be lower than that of PxABCC2 in *P. xylostella*. Indeed, relatively higher reduction in Cry1Ac binding was observed in the ABCC2KO strain than in the ABCC3KO strain. Nevertheless, notably, both the resistance levels to the Cry1Ac toxin and the reduction levels of Cry1Ac binding were substantially lower in the ABCC2KO and ABCC3KO strains than in the near-isogenic resistant NIL-R strain, confirming that the high-level Cry1Ac resistance phenotype in the NIL-R strain is indeed attributable to alterations in multiple midgut receptors in addition to PxABCC2 and PxABCC3. In effect, considering that the PxABCC2 protein can only partially facilitate membrane insertion of pre-pore Cry1Ac oligomers, it has been postulated that other midgut receptors could also favor the membrane insertion of Cry1Ac oligomers in *P. xylostella* (Ocelotl et al., 2017). Hypothetically, these potential midgut receptors may act independently, cooperatively or sequentially to exert proper functions on toxic effects of the Cry1Ac toxin. In this instance, construction of a single knockout *P. xylostella* strain with indel mutations of multiple receptors by CRISPR/Cas9 technology will greatly contribute to providing empirical evidence to elucidate the complex interplay between these midgut receptors.

Toxin-receptor interactions have a substantial impact on the specificity of Bt Cry toxins (Jurat-Fuentes and Crickmore, 2017). Recently, much progress has been made in elucidating the interactions of Bt Cry toxins with insect ABCC2 proteins. In *B. mori*, the extracellular loop 2 (ECL 2) of BmABCC2 is the main region that interacts with domain II of the Cry1Ab and Cry1Ac toxins (Tanaka et al., 2016), whereas

extracellular loop 4 (ECL 4) of BmABCC2 mainly interacts with domain II of the Cry1Aa toxin (Adegawa et al., 2017; Tanaka et al., 2017). In *Spodoptera* species, the extracellular loop 1 (ECL 1) of *S. litura* and *S. frugiperda* ABCC2 is crucial for binding of the Cry1Ac toxin (Liu et al., 2018), while two distinct binding sites for the Cry1A toxins in SeABCC2 of *S. exigua* have been proposed: a common uncharacterized binding site in domain II of the Cry1Ab and Cry1Ac toxins and a different unidentified binding site in domain III of the Cry1Aa and Cry1Ab toxins (Martínez-Solís et al., 2018). Undoubtedly, it will be particularly interesting to further identify and characterize the critical binding regions for specific interactions between PxABCC2/3 and the Cry1Ac toxin.

Previous interstrain allelic complementation tests have identified that the same *BtR-1* resistance locus containing the mutant *PxABCC2* gene confers high-level Cry1Ac resistance in diverse geographic populations of *P. xylostella* including the NIL-R strain (Guo et al., 2015a, 2015c). Although we have discovered the novel MAPK-mediated *trans*-regulation of differential expression of *PxABCC1*, *PxABCC2* and *PxABCC3* genes can result in Cry1Ac resistance in NIL-R strain, the detailed *cis*-mutation sites in the *BtR-1* resistance locus still remain mysterious (Guo et al., 2015a, 2015c). Our allelic complementation test here showed that F1 larvae from both interstrain crosses (ABCC2KO × NIL-R and ABCC3KO × NIL-R) were still resistant to the diagnostic dose of Cry1Ac toxin, implying the NIL-R strain also has mutant *PxABCC2* and *PxABCC3* genes in the *BtR-1* resistance locus, especially the *cis*-mutation of upstream promoter regions accounting for the dramatically reduced expression levels of both genes. On this basis, we can hypothesize that the *cis*-mutation of upstream promoter regions of *PxABCC2* and *PxABCC3* genes might alter the binding of some MAPK-modulated insect transcription factors (TFs) (Guo et al., 2018) thereby reducing the transcription of both genes. Obviously, what and how these *cis*-mutation sites and the corresponding TFs control the decreased expression of *PxABCC2* and *PxABCC3* genes bear further exploration.

In summary, in this study, we successfully knocked out both the *PxABCC2* and *PxABCC3* genes by the CRISPR/Cas9 system and confirmed the important roles of these genes in the Cry1Ac resistance of *P. xylostella*. This work lays the foundation for understanding how Bt Cry toxins use these paralogous ABCC transporters as midgut functional receptors in insects, which will aid in the engineering of the susceptibility to Bt Cry toxins and maintain the high efficacy of Bt sprays and Bt crops.

Acknowledgments

This work was supported by the National Natural Science Foundation of China (31630059; 31701813), the Beijing Key Laboratory for Pest Control and Sustainable Cultivation of Vegetables and the Science and Technology Innovation Program of the Chinese Academy of Agricultural Sciences (CAAS-ASTIP-IVFCAAS).

Appendix A. Supplementary data

Supplementary data to this article can be found online at https://doi.org/10.1016/j.ibmb.2019.01.009.

References

Adang, M.J., Crickmore, N., Jurat-Fuentes, J.L., 2014. Diversity of *Bacillus thuringiensis* crystal toxins and mechanism of action. Adv. Insect Physiol. 47, 39–87.

Adegawa, S., Nakama, Y., Endo, H., Shinkawa, N., Kikuta, S., Sato, R., 2017. The domain II loops of *Bacillus thuringiensis* Cry1Aa form an overlapping interaction site for two *Bombyx mori* larvae functional receptors, ABC transporter C2 and cadherin-like receptor. Biochim. Biophys. Acta 1865, 220–231.

Atsumi, S., Miyamoto, K., Yamamoto, K., Narukawa, J., Kawai, S., Sezutsu, H., Kobayashi, I., Uchino, K., Tamura, T., Mita, K., Kadono-Okuda, K., Wada, S., Kanda, K., Goldsmith, M.R., Noda, H., 2012. Single amino acid mutation in an ATP-binding cassette transporter gene causes resistance to Bt toxin Cry1Ab in the silkworm, *Bombyx mori*. Proc. Natl. Acad. Sci. U.S.A. 109, E1591–E1598.

Ayra-Pardo, C., Raymond, B., Gulzar, A., Rodriguez-Cabrera, L., Moran-Bertot, I., Crickmore, N., Wright, D.J., 2015. Novel genetic factors involved in resistance to *Bacillus thuringiensis* in *Plutella xylostella*. Insect Mol. Biol. 24, 589–600.

Banerjee, R., Hasler, J., Meagher, R., Nagoshi, R., Hietala, L., Huang, F., Narva, K., Jurat-Fuentes, J.L., 2017. Mechanism and DNA-based detection of field-evolved resistance to transgenic Bt corn in fall armyworm (*Spodoptera frugiperda*). Sci. Rep. 7, 10877.

Baxter, S.W., Badenes-Pérez, F.R., Morrison, A., Vogel, H., Crickmore, N., Kain, W., Wang, P., Heckel, D.G., Jiggins, C.D., 2011. Parallel evolution of *Bacillus thuringiensis* toxin resistance in Lepidoptera. Genetics 189, 675–679.

Bravo, A., Likitvivatanavong, S., Gill, S.S., Soberón, M., 2011. *Bacillus thuringiensis*: a story of a successful bioinsecticide. Insect Biochem. Mol. Biol. 41, 423–431.

Crickmore, N., 2016. *Bacillus thuringiensis* resistance in *Plutella*—too many trees? Curr. Opin. Insect Sci. 15, 84–88.

Endo, H., Tanaka, S., Adegawa, S., Ichino, F., Tabunoki, H., Kikuta, S., Sato, R., 2018. Extracellular loop structures in silkworm ABCC transporters determine their specificities for *Bacillus thuringiensis* Cry toxins. J. Biol. Chem. 293, 8569–8577.

Endo, H., Tanaka, S., Imamura, K., Adegawa, S., Kikuta, S., Sato, R., 2017. Cry toxin specificities of insect ABCC transporters closely related to lepidopteran ABCC2 transporters. Peptides 98, 86–92.

Flagel, L., Lee, Y.W., Wanjugi, H., Swarup, S., Brown, A., Wang, J., Kraft, E., Greenplate, J., Simmons, J., Adams, N., Wang, Y., Martinelli, S., Haas, J.A., Gowda, A., Head, G., 2018. Mutational disruption of the ABCC2 gene in fall armyworm, *Spodoptera frugiperda*, confers resistance to the Cry1Fa and Cry1A.105 insecticidal proteins. Sci. Rep. 8, 7255.

Furlong, M.J., Wright, D.J., Dosdall, L.M., 2013. Diamondback moth ecology and management: problems, progress and prospects. Annu. Rev. Entomol. 58, 517–541.

Gahan, L.J., Pauchet, Y., Vogel, H., Heckel, D.G., 2010. An ABC transporter mutation is correlated with insect resistance to *Bacillus thuringiensis* Cry1Ac toxin. PLoS Genet. 6, e1001248.

Guo, Z., Kang, S., Chen, D., Wu, Q., Wang, S., Xie, W., Zhu, X., Baxter, S.W., Zhou, X., Jurat-Fuentes, J.L., Zhang, Y., 2015a. MAPK signaling pathway alters expression of midgut ALP and ABCC genes and causes resistance to *Bacillus thuringiensis* Cry1Ac toxin in diamondback moth. PLoS Genet. 11, e1005124.

Guo, Z., Kang, S., Zhu, X., Wu, Q., Wang, S., Xie, W., Zhang, Y., 2015b. The midgut cadherin-like gene is not associated with resistance to *Bacillus thuringiensis* toxin Cry1Ac in *Plutella xylostella* (L.). J. Invertebr. Pathol. 126, 21–30.

Guo, Z., Kang, S., Zhu, X., Xia, J., Wu, Q., Wang, S., Xie, W., Zhang, Y., 2015c. Down-regulation of a novel ABC transporter gene (*Pxwhite*) is associated with Cry1Ac resistance in the diamondback moth, *Plutella xylostella* (L.). Insect Biochem. Mol. Biol. 59, 30–40.

Guo, Z., Kang, S., Zhu, X., Xia, J., Wu, Q., Wang, S., Xie, W., Zhang, Y., 2015d. The novel ABC transporter ABCH1 is a potential target for RNAi-based insect pest control and resistance management. Sci. Rep. 5, 13728.

Guo, Z., Qin, J., Zhou, X., Zhang, Y., 2018. Insect transcription factors: a landscape of their structures and biological functions in *Drosophila* and beyond. Int. J. Mol. Sci. 19, 3691.

Heckel, D.G., 2012. Learning the ABCs of Bt: ABC transporters and insect resistance to *Bacillus thuringiensis* provide clues to a crucial step in toxin mode of action. Pestic. Biochem. Physiol. 104, 103–110.

Hsu, P.D., Lander, E.S., Zhang, F., 2014. Development and applications of CRISPR-Cas9 for genome engineering. Cell 157, 1262–1278.

ISAAA, 2017. Global Status of Commercialized Biotech/GM Crops in 2017: Biotech Crop Adoption Surges as Economic Benefits Accumulate in 22 Years. *ISAAA Brief* No. 53. ISAAA, Ithaca, NY.

Jinek, M., Chylinski, K., Fonfara, I., Hauer, M., Doudna, J.A., Charpentier, E., 2012. A programmable dual-RNA-guided DNA endonuclease in adaptive bacterial immunity. Science 337, 816–821.

Jurat-Fuentes, J.L., Crickmore, N., 2017. Specificity determinants for Cry insecticidal proteins: insights from their mode of action. J. Invertebr. Pathol. 142, 5–10.

Knott, G.J., Doudna, J.A., 2018. CRISPR-Cas guides the future of genetic engineering. Science 361, 866–869.

Lei, Y., Zhu, X., Xie, W., Wu, Q., Wang, S., Guo, Z., Xu, B., Li, X., Zhou, X., Zhang, Y., 2014. Midgut transcriptome response to a Cry toxin in the diamondback moth, *Plutella xylostella* (Lepidoptera: Plutellidae). Gene 533, 180–187.

Liu, L., Chen, Z., Yang, Y., Xiao, Y., Liu, C., Ma, Y., Soberón, M., Bravo, A., Yang, Y., Liu, K., 2018. A single amino acid polymorphism in ABCC2 loop 1 is responsible for differential toxicity of *Bacillus thuringiensis* Cry1Ac toxin in different *Spodoptera* (Noctuidae) species. Insect Biochem. Mol. Biol. 100, 59–65.

Liu, Y.B., Tabashnik, B.E., 1997. Inheritance of resistance to the *Bacillus thuringiensis* toxin Cry1C in the diamondback moth. Appl. Environ. Microbiol. 63, 2218–2223.

Martínez-Solís, M., Pinos, D., Endo, H., Portugal, L., Sato, R., Ferré, J., Herrero, S., Hernández-Martínez, P., 2018. Role of *Bacillus thuringiensis* Cry1A toxins domains in the binding to the ABCC2 receptor from *Spodoptera exigua*. Insect Biochem. Mol. Biol. 101, 47–56.

Ocelotl, J., Sánchez, J., Gómez, I., Tabashnik, B.E., Bravo, A., Soberón, M., 2017. ABCC2 is associated with *Bacillus thuringiensis* Cry1Ac toxin oligomerization and membrane insertion in diamondback moth. Sci. Rep. 7, 2386.

Pardo-López, L., Soberón, M., Bravo, A., 2013. *Bacillus thuringiensis* insecticidal three-domain Cry toxins: mode of action, insect resistance and consequences for crop protection. FEMS Microbiol. Rev. 37, 3–22.

Park, Y., Gonzalez-Martinez, R.M., Navarro-Cerrillo, G., Chakroun, M., Kim, Y., Ziarsolo, P., Blanca, J., Canizares, J., Ferre, J., Herrero, S., 2014. ABCC transporters mediate insect resistance to multiple Bt toxins revealed by bulk segregant analysis. BMC Biol. 12, 46.

Peterson, B., Bezuidenhout, C.C., Van den Berg, J., 2017. An overview of mechanisms of Cry toxin resistance in lepidopteran insects. J. Econ. Entomol. 110, 362–377.

Pigott, C.R., Ellar, D.J., 2007. Role of receptors in *Bacillus thuringiensis* crystal toxin activity. Microbiol. Mol. Biol. Rev. 71, 255–281.

Schnepf, E., Crickmore, N., Van Rie, J., Lereclus, D., Baum, J., Feitelson, J., Zeigler, D.R., Dean, D.H., 1998. *Bacillus thuringiensis* and its pesticidal crystal proteins. Microbiol. Mol. Biol. Rev. 62, 775–806.

Sun, D., Guo, Z., Liu, Y., Zhang, Y., 2017. Progress and prospects of CRISPR/Cas systems in insects and other arthropods. Front. Physiol. 8, 608.

Tabashnik, B.E., Carrière, Y., 2017. Surge in insect resistance to transgenic crops and prospects for sustainability. Nat. Biotechnol. 35, 926–935.

Tabashnik, B.E., Cushing, N.L., Finson, N., Johnson, M.W., 1990. Field development of resistance to *Bacillus thuringiensis* in diamondback moth (Lepidoptera: Plutellidae). J. Econ. Entomol. 83, 1671–1676.

Tanaka, S., Endo, H., Adegawa, S., Iizuka, A., Imamura, K., Kikuta, S., Sato, R., 2017. *Bombyx mori* ABC transporter C2 structures responsible for the receptor function of *Bacillus thuringiensis* Cry1Aa toxin. Insect Biochem. Mol. Biol. 91, 44–54.

Tanaka, S., Miyamoto, K., Noda, H., Endo, H., Kikuta, S., Sato, R., 2016. Single amino acid insertions in extracellular loop 2 of *Bombyx mori* ABCC2 disrupt its receptor function for *Bacillus thuringiensis* Cry1Ab and Cry1Ac but not Cry1Aa toxins. Peptides 78, 99–108.

Tanaka, S., Miyamoto, K., Noda, H., Jurat-Fuentes, J.L., Yoshizawa, Y., Endo, H., Sato, R., 2013. The ATP-binding cassette transporter subfamily C member 2 in *Bombyx mori* larvae is a functional receptor for Cry toxins from *Bacillus thuringiensis*. FEBS J. 280, 1782–1794.

Wang, J., Zhang, H., Wang, H., Zhao, S., Zuo, Y., Yang, Y., Wu, Y., 2016. Functional validation of cadherin as a receptor of Bt toxin Cry1Ac in *Helicoverpa armigera* utilizing the CRISPR/Cas9 system. Insect Biochem. Mol. Biol. 76, 11–17.

Xia, J., Guo, Z., Yang, Z., Zhu, X., Kang, S., Yang, X., Yang, F., Wu, Q., Wang, S., Xie, W., Xu, W., Zhang, Y., 2016. Proteomics-based identification of midgut proteins correlated with Cry1Ac resistance in *Plutella xylostella* (L.). Pestic. Biochem. Physiol. 132, 108–117.

Xiao, Y., Zhang, T., Liu, C., Heckel, D.G., Li, X., Tabashnik, B.E., Wu, K., 2014. Mis-splicing of the ABCC2 gene linked with Bt toxin resistance in *Helicoverpa armigera*. Sci. Rep. 4, 6184.

Xie, W., Lei, Y., Fu, W., Yang, Z., Zhu, X., Guo, Z., Wu, Q., Wang, S., Xu, B., Zhou, X., Zhang, Y., 2012. Tissue-specific transcriptome profiling of *Plutella xylostella* third instar larval midgut. Int. J. Biol. Sci. 8, 1142–1155.

Zhu, X., Lei, Y., Yang, Y., Baxter, S.W., Li, J., Wu, Q., Wang, S., Xie, W., Guo, Z., Fu, W., Zhang, Y., 2015. Construction and characterisation of near-isogenic *Plutella xylostella* (Lepidoptera: Plutellidae) strains resistant to Cry1Ac toxin. Pest Manag. Sci. 71, 225–233.

Zhu, X., Xie, S., Armengaud, J., Xie, W., Guo, Z., Kang, S., Wu, Q., Wang, S., Xia, J., He, R., Zhang, Y., 2016a. Tissue-specific proteogenomic analysis of *Plutella xylostella* larval midgut using a multi-algorithm pipeline. Mol. Cell. Proteomics 15, 1791–1807.

Zhu, X., Yang, Y., Wu, Q., Wang, S., Xie, W., Guo, Z., Kang, S., Xia, J., Zhang, Y., 2016b. Lack of fitness costs and inheritance of resistance to *Bacillus thuringiensis* Cry1Ac toxin in a near-isogenic strain of *Plutella xylostella* (Lepidoptera: Plutellidae). Pest Manag. Sci. 72, 289–297.